Available online at www.sciencedirect.com
ScienceDirect
Progress in Natural Science 18 (2008) 431–439
Progress in Natural Science
www.elsevier.com/locate/pnsc

Petrology and mineral chemistry of new ureilites found in Grove Mountains, Antarctica

Bingkui Miao [a,b,*], Yangting Lin [b], Guiqin Wang [c], Daode Wang [c], Ziyuan Ouyang [d]

[a] *Key Laboratory of Geological Engineering Center of Guangxi Province, Guilin University of Technology, Guilin 541004, China*
[b] *State Key Laboratory of Lithospheric Evolution, Institute of Geology and Geophysics, Chinese Academy of Sciences, Beijing 100029, China*
[c] *Key Laboratory of Isotope Geochronology and Geochemistry, Guangzhou Institute of Geochemistry, Chinese Academy of Sciences, Guangzhou 510640, China*
[d] *National Astronomical Observatories, Chinese Academy of Sciences, Beijing 100012, China*

Received 26 July 2007; received in revised form 16 August 2007; accepted 9 October 2007

Abstract

Petrography and mineral chemistry of two new ureilites, GRV 021512 and 022931, from the Grove Mountains, Antarctica, are reported in this paper. GRV 021512 exhibits a typical ureilite texture, and consists of 48.3% olivine, 9.4% pigeonite and 38.1% carbonaceous interstitial material and/or reduction product. GRV 022931 has a cataclastic porphyritic texture, and consists of 19.1% olivine and 14.1% pigeonite embedded in 66.3% carbonaceous interstitial material and/or reduction product. The coarse-grained olivine and pigeonite in both meteorites have homogeneous cores, and they are FeO-rich within the range of the ferroan subgroup (subgroup I) of olivine-pigeonite ureilites. All olivine grains of the meteorites show reduction zones along boundaries and cracks. Abundant diamond coexists with graphite as graphite-rich patches and veins in the carbonaceous interstitial material. Petrogenesis of both meteorites and the origin of diamond are discussed.

Keywords: Meteorite; Achondrite; Ureilite; Diamond; Antarctica

Ureilites are ultramafic rocks, consisting mainly of olivine and pigeonite [1]. Augite was found in some of them, and these meteorites are referred to as augite-bearing ureilites [2,3]. In addition, a few ureilites contain other mineral and lithic clasts that are usually feldspathic, and they are classified as polymict ureilites [4–7]. The most abundant olivine-pigeonite ureilites can further be divided into three subgroups mainly based on FeO-contents of olivine and pigeonite [8]. Most ureilites contain various masses of typical fine-grained carbonaceous interstitial material, with identification of amorphous carbon, graphite and diamond. Another unique feature of ureilites is reduction of coarse-grained olivine that has FeO-poor zones with abundant tiny inclusions of Ni-poor metal [9,10].

As achondrites, ureilites show many "igneous" characteristics, including various igneous textures, highly fractionated lithophile elements with enrichment in Sc, V, Mg, Cr and Mn and depletion in Al and Na [11,12] and the V-shaped REE patterns with extreme depletion of middle REE [11,13]. On the other hand, ureilites show various "primitive" features as chondritic meteorites. Oxygen isotopic compositions of ureilites plot on the carbonaceous chondrite anhydrous mineral (CCAM) line with a wide range of $\Delta^{17}O$ [14], which is referred to as a mixing line of the solar nebular and/or interstellar components [15,16]. Other "primitive" features are large abundance of

* Corresponding author. Tel./fax: +86 773 5896108.
E-mail addresses: miaobk@glite.edu.cn, miaobk@mail.igcas.ac.cn (B. Miao).

1002-0071/$ - see front matter © 2007 National Natural Science Foundation of China and Chinese Academy of Sciences. Published by Elsevier Limited and Science in China Press. All rights reserved.
doi:10.1016/j.pnsc.2007.10.009

carbon, planetary noble gases [17,18], and relatively high and unfractionated siderophile element abundances [19–21].

Origins of ureilites can be divided into two models: (1) ultramafic igneous cumulates and (2) residues of partial melting. A line of evidence for the cumulate model is the foliation and lineation of silicate minerals in ureilites [9,22]. Goodrich et al. [23] proposed a multi-stage cumulate model that ureilites are magmatic cumulates deposited from melts generated by low-degree partial melting. This model is consistent with HREE patterns, Eu anomalies, Mn/Mg ratios and superchondritic Ca/Al ratios of ureilites. In contrast, the coexistence of "igneous" and "primitive" features is in general consistent with the residue model [24,25]. Another issue is the origin of diamond in ureilites. Shock-induced conversion of diamond from graphite is commonly accepted [26]. However, recent analyses of C, N and noble gas isotopic compositions do not favor the shock model [27,28]. Another possibility is chemical vapor deposition (CVD) [29].

As a part of the project of classifying 51 representative meteorites of the new 4448 Grove Mountains meteorites collected during 2002—2003 by the 19th Chinese Antarctic Research Expedition, we conducted a petrographic study on two ureilites selected from these samples, and report the results here.

1. Samples and experiments

GRV 021512 is a hemisphere-shaped fragment with a size of 40 mm × 44 mm × 65 mm and it weighs 143.42 g. Most of the fusion crust was broken off. The crust-free surface is dyed in brown, consisting of greenish coarse-grained crystals (olivine) and dark fine-grained interstitial materials. GRV 022931 is a small fragment (1.24 g, 11 mm × 15 mm) without any fusion crust remained. This fragment is heavily weathered, with dark brown color. A small piece of the sample was chiseled off from GRV 022931, and another piece was cut off from GRV 021512. The pieces of samples were embedded in epoxy, and cut into thin slices. A polished thin section (PTS) was made from one of the slices for each meteorite. Petrography was observed both under optical microscopy and in back-scattered electron (BSE) image mode of an electron probe microanalyzer (EPMA) JEOL JXA-8100 in Guangzhou Institute of Geochemistry, Chinese Academy of Sciences. Modal abundances of minerals and the fine-grained interstitial material and/or reduction product are determined from their areas on the BSE images. Quantitative analyses of minerals were conducted using another EPMA type JXA-8800R in Sun Yat-sen University, Guangzhou, with an accelerating voltage of 15 kV and a beam current of 20 nA. The standards are natural and synthetic minerals. Analyses data were treated using the Bence–Albee method. Raman spectra were measured by a Renishaw RM2000 micro laser Raman spectrometer in the Guangzhou Institute of Geochemistry, Chinese Academy of Sciences, Guangzhou. The 785-nm line of the Renishaw semiconductor laser was focused to an area of ~1 μm on samples. The spectra were accumulated for 20 s to enhance signal-to-noise ratio.

2. Results

2.1. Petrography

2.1.1. GRV 021512

The PTS of GRV 021512 is 14 mm × 18 mm in size. There is only a small piece of fusion crust (5.4 mm × 0.3–0.5 mm). GRV 021512 has a typical monomict ureilite texture, composed mainly of equigranular olivine (48.3%), pigeonite (9.4%) and fine-grained carbonaceous interstitial material and/or reduction product (38.1%) (Fig. 1(a)). Grain sizes of the olivine and pigeonite usually range from 0.3 to 2.5 mm with the largest up to 3.5 mm. Pigeonite heterogeneously distributes along the rim of the section, but it may be a result of sampling. Both the coarse-grained olivine and pigeonite are anhedral in shape, and often show triple junctions with 120° angles (Fig. 1(e)). All olivine grains have reduced zones of 20–30 μm wide, which are FeO-poor and contain abundant tiny grains of Ni-poor metal and sulfides. Pigeonite has no significant features of reduction. The carbonaceous interstitial material and/or reduction product have two distinct assemblages (Fig. 1(a) and (c)); most of them (86.5%) are fine-grained mixtures of forsterite, enstatite, low-Ni metal and sulfides, and the less abundant (13.5%) are graphite-rich assemblages as patches and veins (from 0.1 × 0.1 mm to 0.3 × 0.7 mm). The graphite veins are black under reflective light which is distinguished from the normal graphite with bright metallic luster. In graphite veins, abundant diamond grains have been identified by the laser Raman spectra (Fig. 2). It occurs as isolated fine-grained (3–10 μm) grains, and always coexists with graphite (Fig. 3(a)). A few graphite-rich veins penetrate into olivine and pigeonite. The coarse-grained olivine and pigeonite in GRV 021512 are heavily fractured. In addition, they show undulatory extinction in cross-polarized light. Some grains of olivines display planar fractures. Limonite mainly occurs as veins (10–30 μm wide) along silicate boundaries, which are likely weathering products of metal and/or sulfides.

2.1.2. GRV 022931

The PTS of GRV 022931 is 4 mm × 8 mm in size, without any fusion crust. It has a cataclastic porphyritic texture, composed of coarse-grained olivine (19.1%) and pigeonite (14.1%) embedded in carbonaceous interstitial material and/or reduction product (66.3%) (Fig. 1(b)). Both olivine and pigeonite are irregular in shape with embayed outlines (Fig. 1(d)). Olivine shows similar reduced features as that in GRV 021512, but the reduced zones are much wider (up to 100 μm). Furthermore, the reduction along cracks in crystals of olivine is highly developed. Pigeonite does not have the reduction zones.

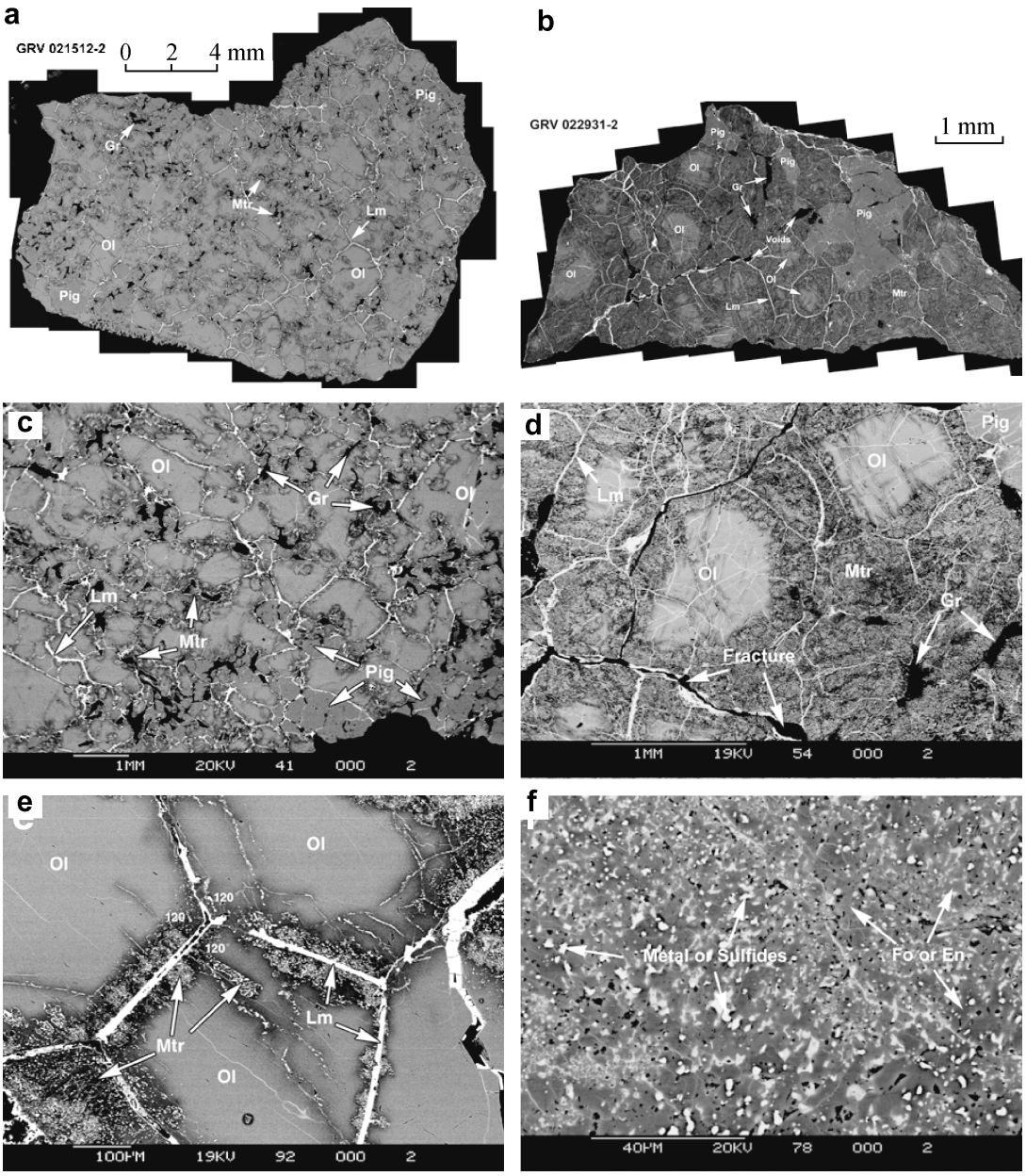

Fig. 1. Backscattered electron (BSE) images of the ureilites. (a) Photomosaic of GRV 021512, consisting of coarse-grained anhedral olivine (Ol) and pigeonite (Pig) with interstitial materials referred to as carbonaceous interstitial (Mtr). Note occurrence of dark pockets and veins of graphite-rich assemblages (Gr). Bright gray veins are weathering products consisting main of limonite (Lm). (b) Photomosaic of GRV 022931, having a similar mineral assemblage like GRV 021512 but with much more abundant carbonaceous interstitial. (c) Inset of GRV 021512, showing textural relationship of the coarse-grained silicates and the carbonaceous interstitial. Note the embayed boundaries of olivine. (d) Inset of GRV 022931, showing a detailed texture of this meteorite. Note eroded boundaries of olivine and many dark gray veins penetrating into the crystals. (e) Inset of GRV 021512, demonstrating triple junctions of the coarse-grained silicates and dark gray reduced zones. Bright tiny grains are opaque minerals (Ni-poor metal and sulfides). (f) Inset of GRV 022931, showing mineral assemblages of the carbonaceous interstitial. Besides metal and sulfides (white), fine-grained silicates are forsterite (Fo) and enstatite (En) (not distinguished here).

The carbonaceous interstitial material and/or reduction product (Fig. 1(b) and (d)) is similar to that in GRV 021512, consisting predominantly of fine-grained mixtures of forsterite, enstatite and opaque minerals (Ni-poor metal, sulfides) (Fig. 1(f)), and less abundant graphite-rich assemblages as patches and veins (Fig. 1(b) and (d)). Abundant fine-grained (1–3 μm) subhedral to euhedral diamond (Fig. 3(b)) was also found in the graphite-rich assemblages. The identification of both diamond and graphite is confirmed by the laser Raman spectra (Fig. 2). Similar to GRV 021512, olivine and pyroxene are fractured, and show undulatory extinction. Weathered products are mainly limonite, filling most of the cracks (Fig. 1(b)).

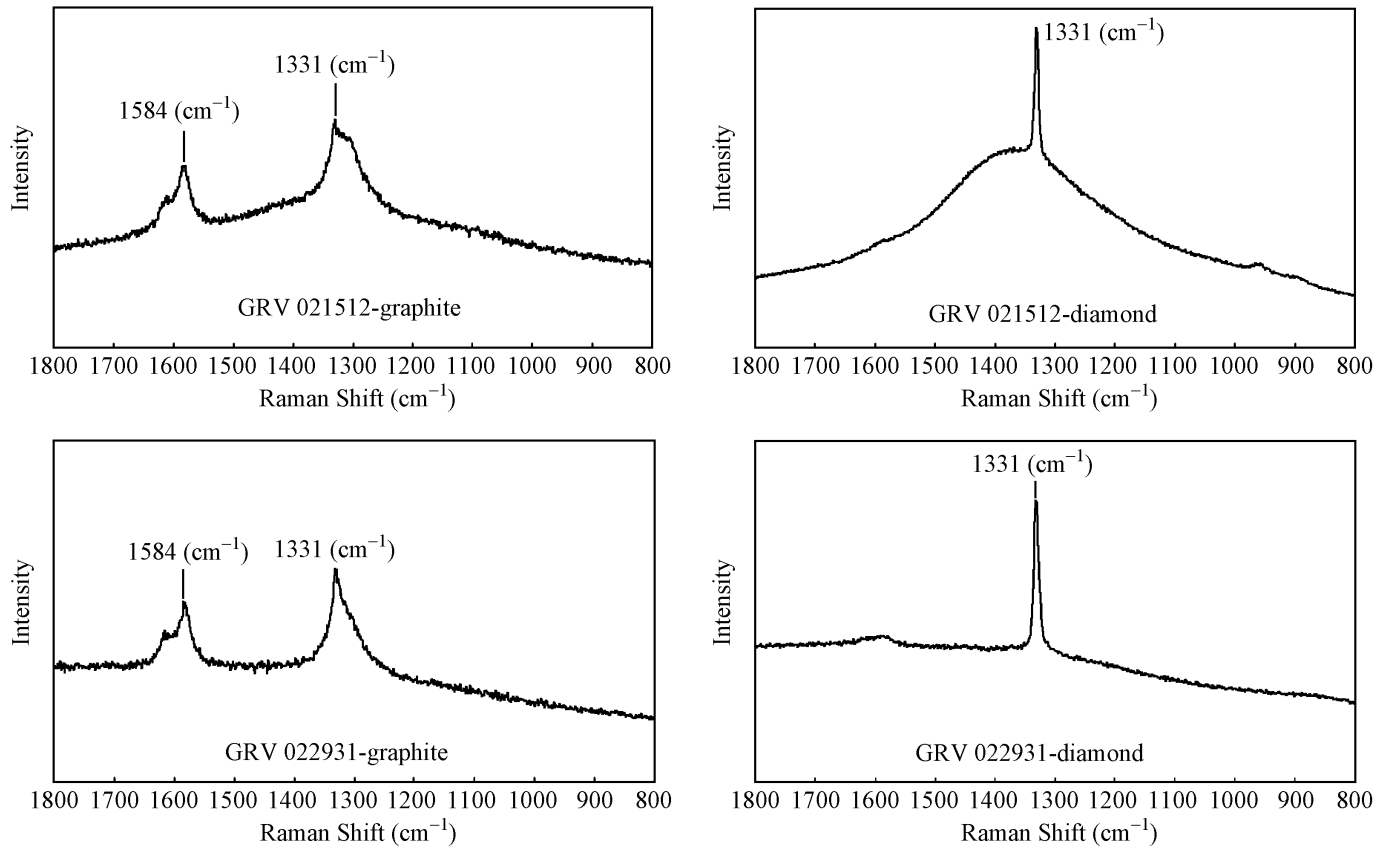

Fig. 2. Micro Raman spectra of graphite and diamond from GRV 021512 and 022931. Diamond shows a single strong peak at 1331 cm^{-1}, whereas graphite has two main peaks at 1331 and 1584 cm^{-1}.

3. Mineral chemistry

3.1. Olivine

The coarse-grained olivines in both meteorites have homogeneous cores, and their forsterite (Fo) contents are nearly identical (GRV 021512: $Fo_{79.6\pm0.2}$; GRV 022931: $Fo_{78.8\pm0.8}$). The Fo contents in the reduced zones increase to 93.4 mol % at the rims in GRV 021512 and to 92.9 mol % in GRV 022931 (Fig. 4). The coarse-grained olivines are typical of Cr_2O_3 and CaO-rich in both GRV 021512 (0.46–0.87% Cr_2O_3, 0.11–0.46% CaO) and GRV 022931 (0.59–2.11% Cr_2O_3, 0.31–0.70% CaO). Other minor element is MnO (GRV 021512: 0.40–0.59%; GRV 022931: 0.43–0.63%). Regardless of the zoning profiles of FeO, the minor elements are nearly constant from the cores to the rims, except for slightly higher Cr_2O_3 and MnO contents in the reduced zones than in the cores in GRV 022931 (Fig. 5). Composition of olivine is summarized in Table 1.

Fig. 6(a) shows a linear correlation between atomic ratios of Fe/Mn and Fe/Mg, indicating reduction of FeO in the zones. The diagram also demonstrates a nearly constant atomic Mg/Mn ratio (157) of olivine in both meteorites. The atomic Fe/Cr ratio is also positively related with the Fe/Mg ratio, with a constant atomic Mg/Cr ratio of 125 (Fig. 6(b)). Distinguished from the above large crystals, the fine-grained olivine in the carbonaceous interstitial is FeO-poor, with a composition of forsterite (Fo 96.0–98.0). However, the contents of minor CaO, MnO and Cr_2O_3 are similar to those of the coarse-grained olivine (Fig. 5).

3.2. Pyroxenes

The coarse-grained pigeonite is homogeneous in both major and minor elements in the two meteorites, with the average compositions of $En_{74.5\pm0.3}Wo_{8.0\pm0.2}Fs_{17.5\pm0.2}$ in GRV 021512 and $En_{71.7\pm0.3}Wo_{10.4\pm0.2}Fs_{17.9\pm0.2}$ in GRV 022931. The Cr_2O_3 content is 1.04–1.22% in GRV 021512 and 1.09–1.18% in GRV 022931, respectively. Other minor elements are Al_2O_3 (GRV 021512: 0.67–0.80%; GRV 022931: 0.66–0.69%), MnO (GRV 021512: 0.39–0.51%; GRV 022931: 0.44–0.47%) and CaO (GRV 021512: 3.70–4.16%; GRV 022931: 5.06–5.21%) (Fig. 7).

The fine-grained pyroxene in the carbonaceous interstitial in GRV 021512 is enstatite ($En_{92.3-92.6}Wo_{0.7-0.9}Fs_{6.7-6.8}$), with much lower Al_2O_3 (0.06–0.15%) and Cr_2O_3 (0.44–0.48%) in comparison with those of the coarse-grained pigeonite. The MnO content (0.43–0.48%) of the fine-grained enstatite is within the range of the coarse-grained pigeonite.

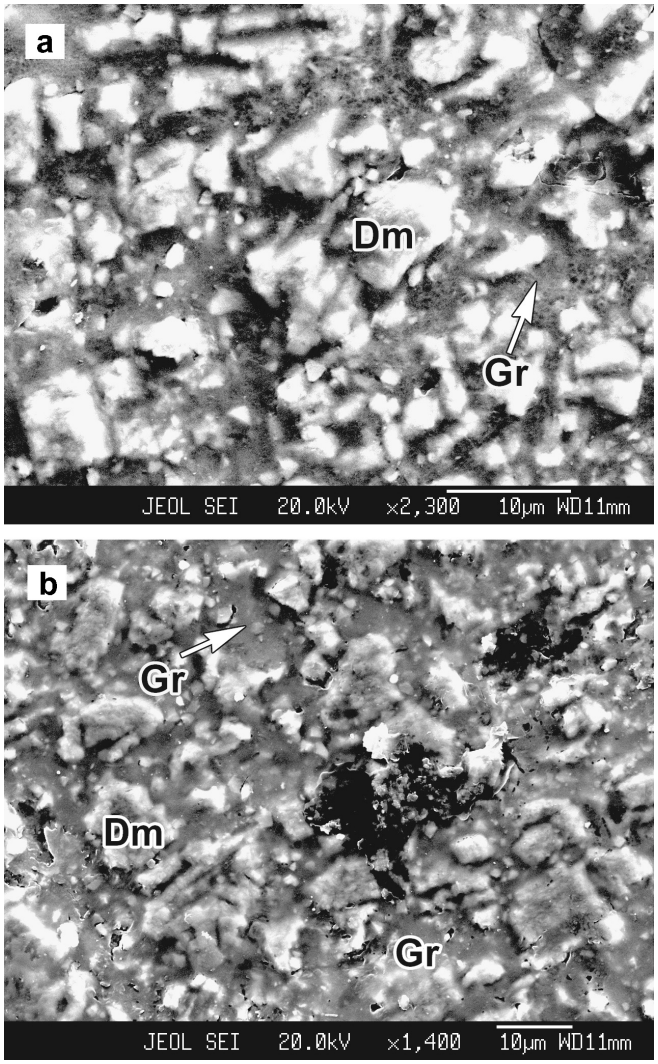

Fig. 3. Second electron images (SEI) of graphite (Gr) and diamond (Dm) in (a) GRV 021512 and (b) GRV 022931. Note diamond as subhedral to euhedral grains with high relief embedding in graphite (low relief) interstitial.

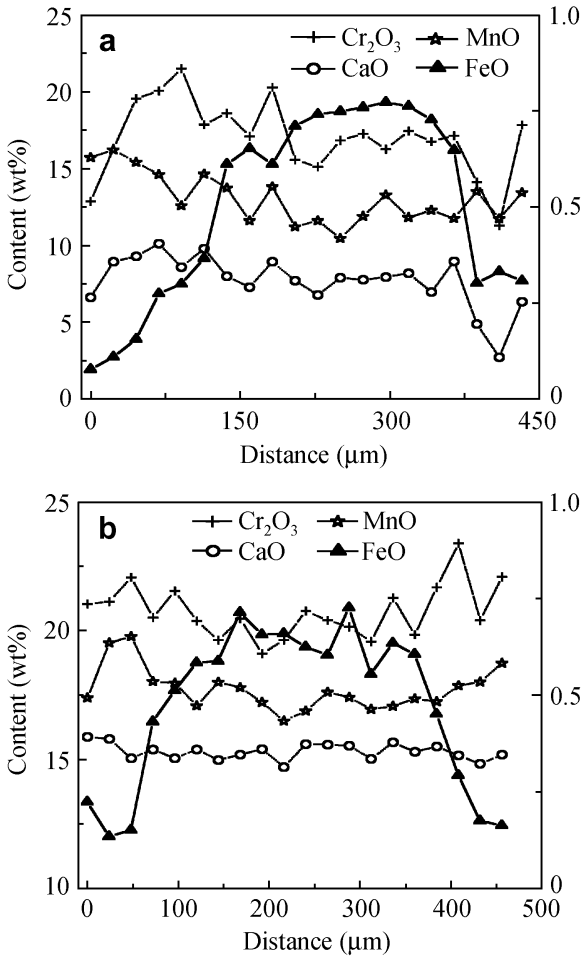

Fig. 4. EPMA profiles of olivine in (a) GRV 021512 and (b) GRV 022931. The olivine grains in both meteorites show reverse zoning with a homogeneous core and a FeO decreasing rim. In contrast, minor CaO, MnO, and Cr_2O_3 are relatively constant.

4. Discussion

4.1. Classification

GRV 021512 shows a typical ureilite texture, composed mainly of coarse-grained anhedral olivine and pigeonite with 120° triple junctions. GRV 022931 contains relict coarse-grained olivine and large crystals of pigeonite in the carbonaceous interstitial without the triple junctions as in GRV 021512, probably due to its very strong reduction. No augite or other lithic clasts were found in the sections, and they are similar to monomict ureilites. Furthermore, the coarse-grained olivine and pigeonite have rather homogeneous cores, and the olivine contains high abundances of CaO and Cr_2O_3. Although the modal abundances of the carbonaceous interstitial are rather different between GRV 021512 and 022931, their mineral assemblages are the same, consisting of fine-grained forsterite, enstatite, Ni-poor metal, sulfides, and various carbon polymorphs. The occurrence of the carbonaceous interstitial is typical of ureilites, especially the olivine-pigeonite type. Another unique feature of the ureilites is the presence of the reduced zones of olivine. Besides along the boundaries of olivine, the reduced zones commonly penetrate inside the crystals especially in GRV 022931.

As shown in Fig. 6, both meteorites have identical Mg/Mn ratios of olivine, which are similar to other monomict ureilites. The coarse-grained olivine and pigeonite in GRV 021512 and 022931 are FeO-rich, within the ranges of the most ferroan subgroup (subgroup I) of olivine-pigeonite ureilites [8,30]. In addition, the coexistence of diamond and graphite reflects that both meteorites experienced strong shock metamorphism. However, most coarse-grained silicates in them are fractured and show undulatory extinction, only a few grains of olivines display planar fractures. Hence, based on the criterion of silicates, the shock stages of both meteorites should be classified as S2/S3 [31].

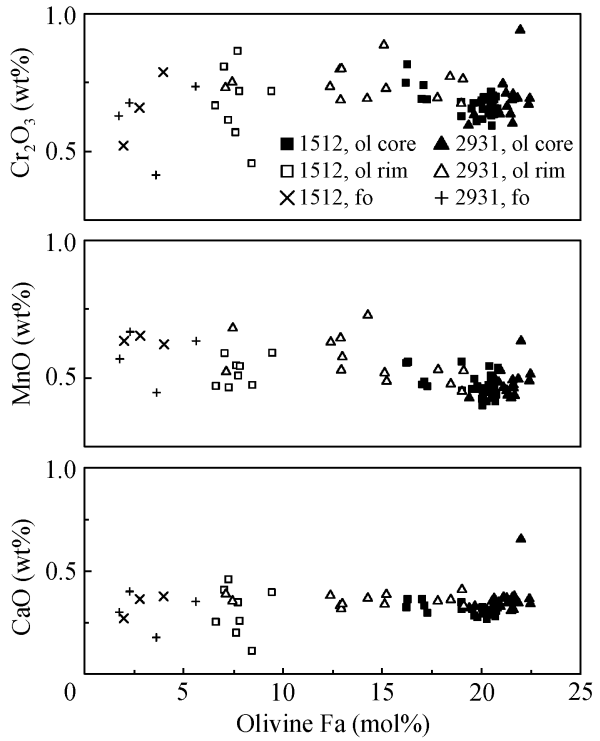

Fig. 5. Compositions of olivine in the ureilites. Regardless of the wide range of fayalite (Fa) content, other minor elements are near constant. Note continuum between the reduced rim and the fine-grained forsterite in the interstitial. Compositions of olivine in GRV 021512 (1512) and GRV 022931 (2931) are indistinguishable.

4.2. Separate or paired?

The nearly identical mineral chemistry and very close find locations (about 18 km away) of GRV 021512 and 022931 suggest a possible pairing, i.e. both meteorites are fragments of a same meteorite fall. However, this possibility can be excluded according to the observed differences in petrography. First, the modal abundance of the carbonaceous interstitial and/or reduction product are much higher in GRV 022931 (66.3%) than in GRV 021512 (38.1%). In fact, the carbonaceous interstitial and/or reduction product are so abundant in GRV 022931 that the coarse-grained olivine and pigeonite are isolated by the former (Fig. 1(b) and (d)). In contrast, the 120° triple junctions of the coarse-grained olivine and pigeonite are preserved in GRV 021512 (Fig. 1(e)). Second, the reduced zones of olivine are significantly wider in GRV 022931 than in GRV 021512 (Fig. 4). In addition, these zones commonly penetrated inside of olivine crystals in GRV 022931. These differences suggest a much higher degree of reduction in GRV 022931 than in GRV 021512. Third, modal abundance ratio of pigeonite/olivine is much higher in GRV 022931 (0.74) than in GRV 021512 (0.19). These differences cannot be related to heterogeneous sampling, but indicate distinct locations in the parent body of ureilites.

4.3. Petrogenesis

Origin of ureilites is a conventional issue. Some authors suggested models that are related with cumulate crystallization of melts generated from low degree melting of plagioclase-depleted sources [9]. In contrast, more workers prefer that ureilites, especially the olivine-pigeonite subtype, are residues of partial melting with at least 15% melt removed from the sources [25]. Our observations favor the residue model too. The presence of the carbonaceous interstitial and/or reduction product is inconsistent with a cumulate origin of the two meteorites. Especially, the very high abundance of the carbonaceous interstitial and/or reduction product in GRV 022931 cannot be explained in the context of any cumulate models. Furthermore, the reduced zones of the coarse-grained olivine suggest subsolidus reduction, consistent with a residue origin instead of cumulate crystallization.

Formation temperatures of the ureilites can be estimated using a geothermometer proposed by Singletary and Grove [25] based on experimental results on melt compositions predicted to be in equilibrium with ureilites. Using their proposed expression and the compositions of pigeonites in GRV 021512 and 022931, temperatures of 1229 and 1217 °C are estimated for the two meteorites, respectively.

After partial melting and removing of the melts, both GRV 021512 and 022931 experienced subsolidus reduction, with FeO-component of the olivine reacted with elemental carbon to form Ni-poor metal. The degree of reduction is probably related with mass of the carbonaceous materials because both GRV 021512 and 022931 have nearly identical mineral compositions. The much higher percentage of the reduced olivine in GRV 022931 than in GRV 021512 is consistent with very abundant carbonaceous materials in the former.

One possible origin of diamond in ureilites is chemical vapor deposition (CVD) [29], which is consistent with non-shock models of diamond based on isotopic data of C, N and noble gases [27,28]. However, the coexistence of diamond with graphite and strongly shocked silicates (S3-S6) indicated the shock-induced origin of diamond [26]. Though the diamond grains in a few ureilites occurred in chains, the diamond grains in both ureilites have similar occurrence and size with diamond in most diamond-bearing ureilites. But the two ureilites have much weaker shock effects (S2/S3) than the other diamond-bearing ureilites in [26]. Absence of severe shock effects in the olivine and pigeonite can be explained by thermal metamorphism after the main shock event. Such a strong thermal metamorphism can also be related to the reduction typical of ureilites. It is noted that numerous reduced zones developed along cracks in olivine especially in GRV 022931, indicating that the thermal metamorphism is posterior to the impact event.

Table 1
Chemical composition of minerals in GRV 021512 and GRV 022931 (wt%)

	GRV 021512										
	Equigranular olivine				Interstitial forsterite		Equigranular pigeonite				Interstitial enstatite
	Core		Rim		Core		Core		Rim		Range
SiO_2	39.2 ± 0.3	*38.8–39.6*	40.6 ± 1.1	*39.1–43.1*	41.1 ± 0.3	*40.9–41.5*	55.0 ± 0.3	*54.4–55.4*	55.2 ± 0.3	*54.7–55.6*	*52.7–55.1*
TiO_2	0.01	*<0.04*	0.01	*<0.05*	0.01	*<0.01*	0.05 ± 0.03	*<0.10*	0.05 ± 0.03	*0.02–0.08*	*0.01–0.02*
Al_2O_3	0.03	*<0.08*	0.03	*<0.10*	0.02	*<0.04*	0.74 ± 0.03	*0.69–0.80*	0.73 ± 0.04	*0.67–0.78*	*0.06–0.15*
Cr_2O_3	0.67 ± 0.03	*0.59–0.74*	0.69 ± 0.11	*0.46–0.87*	0.66 ± 0.13	*0.52–0.79*	1.14 ± 0.05	*1.06–1.22*	1.15 ± 0.06	*1.04–1.21*	*0.44–0.48*
FeO	18.8 ± 0.6	*16.2–19.3*	11.4 ± 4.8	*6.05–18.8*	2.85 ± 0.99	*1.93–3.90*	11.3 ± 0.1	*11.1–11.5*	11.3 ± 0.1	*11.1–11.5*	*4.86–4.99*
MnO	0.46 ± 0.04	*0.40–0.56*	0.51 ± 0.05	*0.44–0.59*	0.64 ± 0.02	*0.62–0.65*	0.45 ± 0.04	*0.39–0.50*	0.45 ± 0.03	*0.40–0.51*	*0.43–0.48*
MgO	41.7 ± 0.6	*41.0–4.2*	47.2 ± 3.5	*42.0–51.2*	53.2 ± 0.6	*52.6–53.7*	27.0 ± 0.3	*26.0–27.3*	27.1 ± 0.2	*26.9–27.3*	*37.3–38.5*
CaO	0.31 ± 0.02	*0.27–0.35*	0.31 ± 0.09	*0.11–0.46*	0.34 ± 0.06	*0.27–0.38*	4.02 ± 0.08	*3.84–4.11*	3.99 ± 0.13	*3.70–4.16*	*0.41–0.51*
Na_2O							0.12 ± 0.04	*0.01–.22*	0.12 ± 0.07	*0.01–.21*	*0.01–0.04*
K_2O							0.00	*<0.01*	0.00	*<0.02*	*0.00–0.01*
Fa	20.2 ± 0.8	*17.1–20.8*	12.0 ± 5.2	*6.60–20.1*	2.92 ± 1.0	*1.97–3.99*					
Fo	79.8 ± 0.8	*79.2–82.9*	88.0 ± 5.2	*79.9–93.4*	97.1 ± 1.0	*96.0–98.0*					
En							74.5 ± 0.3	*73.8–74.9*	74.6 ± 0.4	*74.3–75.4*	*92.3–92.6*
Wo							7.96 ± 0.16	*7.61–8.20*	7.9 ± 0.3	*7.32–8.13*	*0.71–0.91*
Fs							17.5 ± 0.2	*17.2–18.0*	17.5 ± 0.2	*17.2–17.6*	*6.73–6.76*
Anal. points	26		14		3		19		8		*2*

	GRV 022931									
	Equigranular olivine				Interstitial forsterite		Equigranular pigeonite			
	Core		Rim		Core		Core		Rim	
SiO_2	38.4 ± 0.4	*37.1–38.9*	39.1 ± 1.0	*37.6–40.8*	41.2 ± 0.7	*40.4–42.0*	54.2 ± 0.2	*53.9–54.4*	54.4	*54.2–54.5*
TiO_2	0.01	*<0.05*	0.00	*<0.02*	0.01	*<0.02*	0.06 ± 0.02	*0.04–0.09*	0.05	*0.02–0.08*
Al_2O_3	0.03	*<0.06*	0.03	*<0.09*	0.03	*<0.06*	0.68 ± 0.01	*0.66–0.69*	0.69	*0.69*
Cr_2O_3	0.67 ± 0.04	*0.59–0.75*	0.85 ± 0.36	*0.67–2.11*	0.61 ± 0.14	*0.41–0.74*	1.13 ± 0.04	*1.09–1.18*	1.17	*1.13–1.20*
FeO	19.4 ± 0.8	*17.6–20.9*	13.8 ± 3.6	*6.80–19.3*	3.29 ± 1.75	*1.74–5.65*	11.3 ± 0.1	*11.2–11.5*	11.1	*10.9–11.2*
MnO	0.47 ± 0.03	*0.43–0.53*	0.56 ± 0.08	*0.45–0.73*	0.58 ± 0.10	*0.45–0.67*	0.46 ± 0.02	*0.44–0.47*	0.46	*0.42–0.50*
MgO	40.5 ± 0.6	*39.6 ± 42.0*	44.7 ± 3.4	*38.5–49.8*	53.7 ± 0.7	*53.1–54.7*	25.4 ± 0.2	*25.3–25.6*	25.7	*25.5–25.9*
CaO	0.35 ± 0.02	*0.31–0.38*	0.40 ± 0.11	*0.32–0.70*	0.31 ± 0.10	*0.18–0.40*	5.12 ± 0.06	*5.06–5.21*	5.15	*5.11–5.18*
Na_2O							0.06 ± 0.01	*0.05–0.07*	0.07	*0.05–0.09*
K_2O							0.00	*0.00*	<0.01	*0.00–0.01*
Fa	21.2 ± 0.8	*19.4–22.5*	14.9 ± 4.2	*7.12–22.0*	3.31 ± 1.72	*1.75–5.60*				
Fo	78.8 ± 0.8	*77.5–80.6*	85.1 ± 4.2	*78.0–92.9*	96.7 ± 1.7	*94.4–98.3*				
En							71.7 ± 0.3	*71.44–72.1*		*72.2–72.3*
Wo							10.4 ± 0.2	*10.2–10.6*		*10.40*
Fs							17.9 ± 0.2	*17.7–18.1*		*17.3–17.5*
Anal. points	17		15		4		4		*2*	

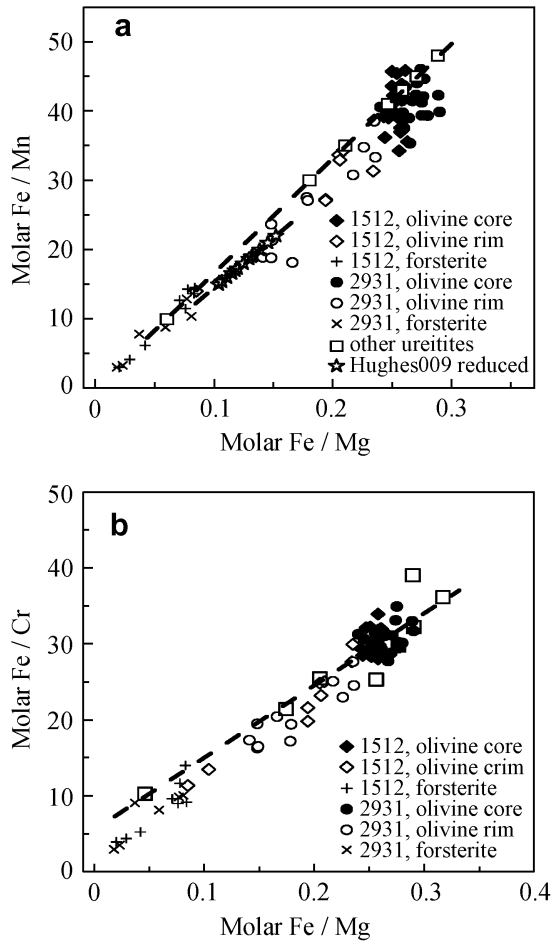

Fig. 6. Atomic ratio correlations of olivine in GRV 021512 and 022931, in comparison with other ureilites. (a) Fe/Mn versus Fe/Mg ratios, showing a linear correlation between them. The compositions of the olivine cores in both meteorites plot at the ferroan end of ureilites. (b) Fe/Cr versus Fe/Mg, showing a similar linear correlation.

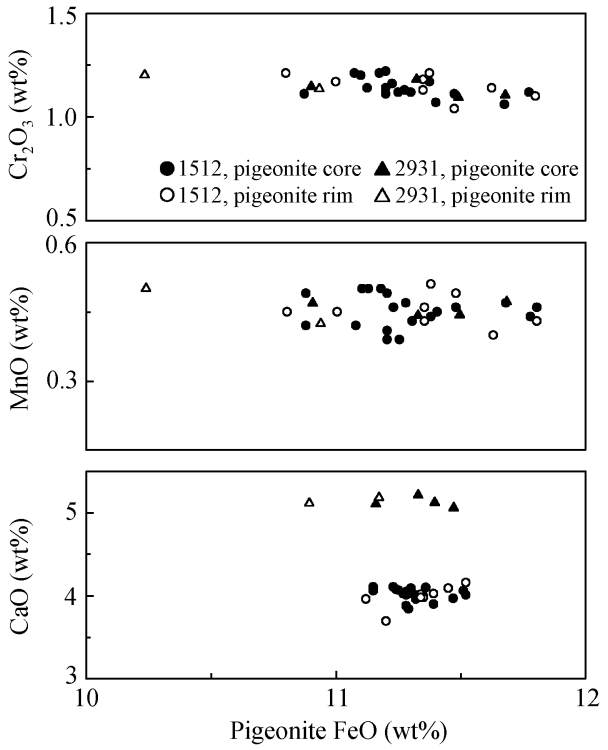

Fig. 7. Compositions of pigeonite in the ureilites. Note relatively homogeneous and identical compositions of pigeonite in GRV 021512 (1512) and GRV 022931 (2931), except for higher CaO in the latter.

5. Conclusions

Both GRV 021512 and 022931 are classified as ureilites of olivine-pigeonite type. They share most unique features of this special group of meteorites, including the mineral assemblages of coarse-grained olivine and pigeonite that usually show 120° triple junctions and have homogeneous compositions in the cores, presence of the abundant carbonaceous interstitial and/or reduction product with graphite and diamond, and the reduction zones along boundaries and cracks of the olivine. The coarse-grained olivine and pigeonite in both meteorites are FeO-rich, with the fayalite content of the olivine and ferrosilite content of pigeonite plotted within the ranges of the ferroan subgroup of olivine-pigeonite ureilites (subgroup I).

Although GRV 021512 and 022931 have nearly identical mineral chemistry and their find sites were close, GRV 022931 has much higher modal abundance of the carbonaceous interstitial and/or reduction product, and shows much higher degree of the reduction in comparison with GRV 021512, excluding possible pairing of them.

Formation temperatures of GRV 021512 and 022931 are determined to be 1229 and 1217 °C, respectively, using a geothermometer. The results are similar with other olivine-pigeonite ureilites. The high abundances of the carbonaceous interstitial and/or reduction product and subsolidus reduction of olivine in our samples are consistent with the residue model of ureilites. Coexistence of abundant diamond with graphite in both meteorites suggests a shock-induced conversion of diamond from graphite. Absence of severe shock effects of silicates could be related a thermal metamorphism posterior to the main impact event.

Acknowledgements

This work was supported by the Pilot Project of Knowledge Innovation of Chinese Academy of Sciences (Grant No. KZCX2-YW-110) and the National Natural Science Foundation of China (Grant Nos. 40473037 and 40673055). The authors thank all the team members (Ju Yitai, Li Jinyan, Xu Xiaxing, Miao Bingkui, Qin Xiang, Yu Liangjun, Yan Li, and Zhang Shengkai) of the 19th CHINARE for collecting 4448 Antarctic meteorites. We are grateful to Li Yuansheng for the help in allocating the samples, and to Chen Linli for laboratory assistances. Discussions and comments from Zhou Xinhua, Liu Xiaohan, and Tao Kejie are helpful. The sample is provided by the Polar Research Institute of China.

References

[1] Mittlefehldt WD, McCoy TJ, Goodrich CA, et al. Non-chondritic meteorites from asteroidal bodies. In: Reviews in mineralogy: planetary materials, vol. 36; 1998. p. 4-1–195.

[2] Goodrich CA, Fioretti AM, Tribaudino M, et al. Primary trapped melt inclusions in olivine in the olivine-augite-orthopyroxene ureilite Hughes 009. Geochim Cosmochim Acta 2001;65:621–52.

[3] Takeda H, Mori H, Ogata H. Mineralogy of augite-bearing ureilites and the origin of their chemical trends. Meteoritics 1989;24:73–81.

[4] Prinz M, Weisberg MK, Nehru CE, et al. North Haig and Nilpena: paired polymict ureilites with Angra DOS reis-related and other clasts. Lunar Planet Inst Conf Abstr 1986;17:681–2.

[5] Ikeda Y, Prinz M. Magmatic inclusions and felsic clasts in the Dar al Gani 319 polymict ureilite. Meteorit Planet Sci 2001;36:481–99.

[6] Jaques AL, Fitzgerald MJ. The Nilpena ureilite, an unusual polymict breccia – implications for origin. Geochim Cosmochim Acta 1982;46:893–900.

[7] Prinz M, Weisberg MK, Nehru CE, et al. EET 83309, a polymict ureilite: recognition of a new group. Lunar Planet Inst Conf Abstr 1987;18:802.

[8] Sinha SK, Sack RO, Lipschutz ME. Ureilite meteorites – equilibration temperatures and smelting reactions. Geochim Cosmochim Acta 1997;61:4235.

[9] Berkley JL, Taylor GJ, Keil K, et al. The nature and origin of ureilites. Geochim Cosmochim Acta 1980;44:1579–97.

[10] Goodrich CA. Ureilites – a critical review. Meteoritics 1992;27:327–52.

[11] Warren PH, Kallemeyn GW. Geochemistry of polymict ureilite EET83309, and a partially-disruptive impact model for ureilite origin. Meteoritics 1989;24:233–46.

[12] Hintenberger H, Jochum KP, Braun O, et al. The Antarctic meteorite Yamato 74123 – a new ureilite. Earth Planet Sci Lett 1978;40:187–93.

[13] Guan Y, Crozaz G. Microdistributions and petrogenetic implications of rare earth elements in polymict ureilites. Meteorit Planet Sci 2001;36:1039–56.

[14] Clayton RN, Mayeda TK. Oxygen isotope studies of achondrites. Geochim Cosmochim Acta 1996;60:1999–2017.

[15] Clayton RN, Grossman L, Mayeda TK. A component of primitive nuclear composition in carbonaceous meteorites. Science 1973;182:485–8.

[16] Clayton RN. Oxygen isotopes in meteorites. Ann Rev Earth Planet Sci 1993;21:115–49.

[17] Goebel R, Ott U, Begemann F. On trapped noble gases in ureilites. J Geophys Res 1978;83:855–67.

[18] Wacker JF. Noble gases in the diamond-free ureilite, ALHA 78019 – the roles of shock and nebular processes. Geochim Cosmochim Acta 1986;50:633–42.

[19] Boynton WV, Starzyk PM, Schmitt RA. Chemical evidence for the genesis of the ureilites, the achondrites Chassigny and the nakhlites. Geochim Cosmochim Acta 1976;40:1439–47.

[20] Goodrich CA, Jones JH, Spitz AH. Siderophile element tests of ureilite petrogenesis models. Meteoritics 1987;22:392.

[21] Wasson JT, Chou C-L, Bild RW, et al. Classification of and elemental fractionation among ureilites. Geochim Cosmochim Acta 1976;40:1449–58.

[22] Berkley JL, Jones JH. Primary igneous carbon in ureilites – petrological implications. J Geophys Res Suppl 1982;87:A353–64.

[23] Goodrich CA, Jones JH, Berkely JL. Origin and evolution of the ureilite parent magmas – multi-stage igneous activity on a large parent body. Geochim Cosmochim Acta 1987;51:2255–73.

[24] Scott ERD, Taylor GJ, Keil K. Origin of ureilite meteorites and implications for planetary accretion. Geophys Res Lett 1993;20:415–8.

[25] Singletary SJ, Grove TL. Early petrologic processes on the ureilite parent body. Meteorit Planet Sci 2003;38:95–108.

[26] Bischoff A, Goodrich CA, Grund T. Shock-induced origin of diamonds in Ureilites. Lunar Planet Inst Conf Abstr 1999;30: 1100.

[27] Rai VK, Murty SVS, Ott U. Nitrogen components in ureilites. Geochim Cosmochim Acta 2003;67:2213–37.

[28] Rai VK, Murty SVS, Ott U. Nitrogen in diamond-free ureilite Allan Hills 78019: clues to the origin of diamond in ureilites. Meteorit Planet Sci 2002;37:1045–55.

[29] Matsuda JI, Fukunaga K, Ito K. Noble gas studies in vapor-growth diamonds – comparison with shock-produced diamonds and the origin of diamonds in ureilites. Geochim Cosmochim Acta 1991;55:2011–23.

[30] Berkley JL, Taylor GJ, Keil K. Ureilites: origin as related magmatic cumulates. Lunar Planet Inst Conf Abstr 1978;9:73–5.

[31] Stoeffler D, Keil K, Scott ERD. Shock metamorphism of ordinary chondrites. Geochim Cosmochim Acta 1991;55:3845–67.